JOURNAL OF AIRCRAFT
Vol. 30, No. 3, May–June 1993

Geometrical and Numerical Considerations in Computing Advanced-Propeller Noise

Valana L. Wells* and Arris Han†
Arizona State University, Tempe, Arizona 85287

A previously developed technique for numerically solving the acoustic analogy equation for rotating surfaces with supersonic regions results in smooth pressure-time waveforms. The method appears to provide results superior to those of other schemes because it eliminates erratic "noise" in the computed waveforms and deals only with nonsingular integrals. This article discusses the application of the method to propeller-type rotor blades. Several different sweep geometries are considered, and presented results show the effect of blade shape on the noise produced and on the numerical procedure for computing that noise. Computed waveforms exhibit expected behavior, deduced from analysis of the retarded blade shapes (acoustic planforms) and the critical points along the blade edges where the Mach number in the direction of the observer equals one.

I. Introduction

THE problem of the linear propagation of rotor and propeller noise has been studied extensively, with fairly good but, as yet, inconclusive results. The methods of Farassat[1] and Hanson[2] appear to provide reliable estimates of the sound pressure levels in the field of advanced propellers with supersonic tips. Nevertheless, the details of the waveforms produced by such surfaces remain somewhat elusive in the sense that the various published results differ from each other. The differences, for the most part, are not in the gross shape and magnitude of the signatures, but are exhibited in the waveforms' secondary characteristics. These discrepancies are attributable to the handling of what will be termed "critical" points in the source integrations. These critical locations have been studied previously from the mathematical point of view.[3–5] Chapman[4] recognized the existence of these critical points and their importance in specifying discontinuities and singularities in the waveform. Amiet,[3] through analysis of the critical locations, devised a method for computing smooth thickness noise waveforms for helicopter-type blades. This article utilizes a previously developed methodology,[5] which takes account of the critical points in the integration, and applies it to the computation of advanced-propeller blade noise. The resulting waveforms, produced by blades with complex geometry, show the same smoothness exhibited by Amiet's results for simple blades. The method used here has the advantage over that of Amiet in that it does not require the numerical solution of singular integrals.

Farassat[6,7] has developed a reformulation of the Ffowcs Williams and Hawkings equation in which the derivatives that operate on the linear sources are taken under the integral sign. His more recent work develops the same type of formulation for the quadrupole sources.[8,9] The latter formulations are appropriate for computing rotor noise when the tip velocity is supersonic. Farassat has taken this approach because, as he points out, the functions in question are sensitive to observer time, particularly near regions where the sources are traveling toward the observer at a Mach number of one, and therefore, numerical time differentiation of them is prone to error. The above observation is true; nevertheless, the authors have shown that by strategic placement of the integration grid, the numerical integration produces a smooth curve which is readily differentiated.[10] The numerical derivative of the acoustic integrals may be taken with as good or better results than those of previous efforts which have moved the derivative inside the integral.

An unfortunate consequence of moving the time derivative inside the integral sign is that the integrand becomes singular when the Mach number of a point on the surface edge in the direction of the observer (M_r) becomes equal to 1. It can be shown that for a real, continuous surface, there will exist at least one such location any time any part of the surface travels at $M_r \geq 1$. There is, therefore, a fairly large range of observer times over which a numerical singular integration must be carried out. Though the singularity is, for the most part, integrable, it does add to the complexity of the numerical procedure. Farassat[1] manipulates the integrand into a form which removes the singular part from the integral. This eliminates the need to handle the singularities numerically. Nonetheless, the inherent nearly singular behavior at these critical points appears to cause the remaining lack of smoothness in his computed waveforms.

It is, however, instructive to take the derivatives inside the integrals in order to perform an analysis of the expected singularities in the resulting acoustic waveform. This has been carried out by Amiet[3] and Chapman,[11] among others, and in a more general way by the current authors.[5,10] Such studies have shown that a rotating surface source with a supersonic tip may produce singular waveforms. The order of singularity depends on the source model(s) such as those describing thickness noise produce logarithmic singularities in the acoustic field. Models which have been used in the past to predict noise using the Lighthill[12] quadrupole integral produce a $1/x$-type singularity. Tam[13] showed that a thickness noise model incorporating a blunt leading edge leads to a singularity in the far field of the $1/\sqrt{x}$-type. Figure 1 illustrates the former two types of singularities for a simple rectangular blade with tip Mach number of 1.5 and an in-plane observer. In this case, the rotor does not experience any axial velocity—that is, the case is representative of a hovering helicopter rotor with supersonic tip.

The above paragraph alludes to the fact that the acoustic waveform may exhibit singular behavior if the surface source has regions which travel supersonically. The previously cited works outline the conditions under which singular points will occur. Simply put, singularities (whether logarithmic or $1/x$)

Presented as Paper 90-3997 at the AIAA 13th Aeroacoustics Conference, Tallahassee, FL, Oct. 22–24, 1990; received April 13, 1991; revision received April 21, 1992; accepted for publication April 21, 1992.

*Assistant Professor, Department of Mechanical and Aerospace Engineering.

†Graduate Student, Department of Mechanical and Aerospace Engineering; currently Research Associate, VPI & SU, NASA Langley Research Center.

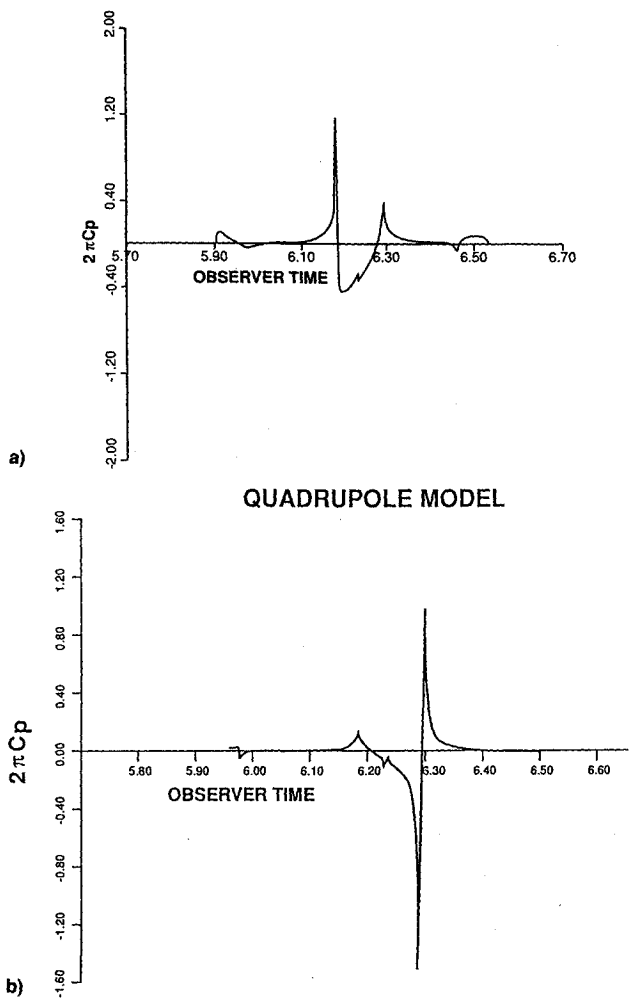

Fig. 1 Acoustic waveforms for rectangular blade, in-plane observer: a) thickness noise source, logarithmic singularity; and b) "quadrupole" noise source, pole singularity.

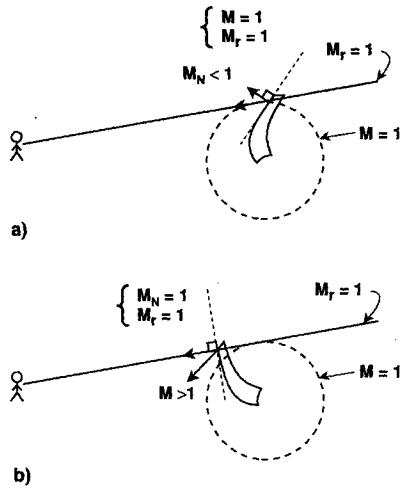

Fig. 2 Conditions for singular behavior of the acoustic waveform: a) $M_{le} = 1$ and $M_r = 1$, no singularity; and b) $M_{N_{le}} = 1$ and $M_r = 1$, singularity produced.

are generated by the moving surface when its edge (leading or trailing) is perpendicular to a line along which $M_r = 1$, where M_r is the Mach number vector component in the direction of the observer. This condition implies that the Mach number perpendicular to the blade, M_N, at the edge is equal to one at the same time that $M_r = 1$. Figure 2 illustrates these necessary conditions for singularity generation. As the figure makes evident, the appearance of singularities depends highly on the geometry of the rotating surface and, in particular, on the leading- and trailing-edge sweep. The figure, evidently, illustrates the conditions for singularity for a rotor with no axial velocity and an in-plane observer. The conditions for the more general case, that of a rotating blade with axial velocity and observer out of plane, are equivalent (but difficult to illustrate because of the three-dimensionality) and are discussed subsequently.

It should be pointed out that the singularities in the waveform will occur only if there is some kind of discontinuity in the curve representing the source value as a function of distance along a coordinate in the direction of motion. In terms of generalized functions, the source strength along this coordinate (s) is equal to $\bar{h}(s)[H(s - s_{te}) - H(s - s_{le})]$, where $\bar{h}(s)$ describes the source strength between the leading and trailing edges, denoted by s_{le} and s_{te}, respectively. The strength is zero elsewhere. Discontinuities in this function generally occur at the leading and trailing edges when considering thickness sources, and at leading, trailing, or shock edges in the case of pressure sources. As an example of the discontinuity to which the above refers, a sharp leading or trailing edge of a cross section of the surface (the blade airfoil) provides a discontinuity in the value of a thickness noise source. (Recall that the thickness noise source is proportional to the normal velocity which, in turn, depends on the slope of the cross section.) A shock wave gives a pressure source which is discontinuous in value, as does the Δp distribution predicted by linear supersonic aerodynamic theory. It is apparent, then, that a cross section with cusped leading and trailing edges will produce no singularities in a thickness noise computation. Similarly, a Δp distribution which goes to zero at leading and trailing edges and is otherwise continuous will produce no singularities in a loading noise computation. It should be noted that the above-discussed singularities are not the same as those discussed by Farassat[14] or, indeed, by Ffowcs Williams and Hawkings.[15] These previous studies analyze a singular point arising from a term which is neglected in the current study. The neglected term can be thought of as a conversion factor between the gradient of the actual surface and the gradient of the retarded (or acoustic planform) surface. Though the term can be important for thick moving bodies, the rotors under study here have small thickness ratio and sharp leading edges which make the conversion approximately equal to one. In cases where the "conversion factor" becomes zero, the source integrals contain a singularity which is shown by Farassat and by Ffowcs Williams and Hawkings to be integrable. Neglecting this factor is similar to making a "thin airfoil" approximation, where sources representing thickness or pressure are distributed over an approximate mean surface rather than the actual rotor surface.

This article discusses a computational procedure which has been effective in producing very smooth acoustic waveforms for rotating surfaces with supersonic tips. The method's success depends on a priori knowledge of the critical point ($M_r = 1$) locations on the leading and trailing edges of the surface. The number of such critical points at any observer time depends highly on the surface geometry. Straight blades, such as helicopter rotor blades, have only one critical point per edge per observer time. Adding sweep to the blade also adds the possibility of multiple critical points. Obviously, the position of these points changes as observer time progresses, and their locations must be computed at each considered time.

II. Solution Methodology

The waveforms are calculated by finding a solution to the wave equation in an acoustic analogy form

$$4\pi\alpha_0^2\rho' = \frac{\partial^n}{\partial x_i \partial x_{j,\ldots}} \int_V \frac{Q_{i,j,\ldots}(y,\tau)}{|x - y|}\, dV(y) \qquad (1)$$

where ρ' is the acoustic density, x represents the observer location and y the source location at the emission time τ.

$Q(y, \tau)$ is the source strength computed at the source location at the emission time, and α_0 represents the ambient speed of sound. If we restrict ourselves to surface sources and to an observer located in the far field, all right-hand terms in the acoustic analogy can be written as having time rather than spatial derivatives, and the equation becomes

$$4\pi p' = \frac{\partial}{\partial t}\int_S \frac{Q(y, \tau)}{\Lambda|x - y|}\, dS(y) \tag{2}$$

where p' is the acoustic pressure and Λ is the conversion factor referred to in Sec. I. For thin surfaces, such as those of the rotors studied here, $\Lambda \approx 1$. In this form, the integral must be taken over the "acoustic planform," i.e., the surface representing the locations of all sources at their emission times. Equation (2) models both thickness and loading noise of a rotor or propeller for an observer located in the far field. The near-field loading term is actually easily included, but, in many cases, it contributes only negligibly, and will not be considered here. It is interesting to note, however, that the near-field term does not contribute to any acoustic singularities. In a mathematical sense, this may be understood by noting that the near-field integral does not have a time derivative operating on it, and, thus, has no mechanism for introducing singular behavior into the waveform as long as the integrand itself is nonsingular. Physically speaking, one realizes that the near-field term does not represent a propagating wave—its contribution is, in fact, often termed "pseudosound."

Dividing Eq. (2) into thickness and far-field loading terms, and making the equation dimensionless leads to the quite familiar result

$$4\pi\tilde{p}' = \frac{\partial}{\partial\tilde{t}}\int_S \frac{Mn}{\tilde{r}}\, d\Sigma + \frac{\partial}{\partial\tilde{t}}\int_S \frac{\tilde{p}_r}{\tilde{r}}\, d\Sigma \tag{3}$$

In the above, tildes indicate dimensionless quantities. Pressures are made dimensionless by the quantity $\rho_0\alpha_0^2$, and all linear dimensions are referred to α_0/Ω, where Ω is the rotor angular velocity. Dimensionless time is equal to Ωt, $M_n = v_n/\alpha_0$, and r is shorthand for $|x - y|$. The differential surface area $d\Sigma$ indicates integration over the dimensionless acoustic planform which, in some references, is termed the Σ surface. The quantity $\tilde{p}_r$ is simply the component of the pressure at the surface, multiplied by the unit normal to the surface in the direction of the observer, i.e., $\tilde{p}_r = \tilde{p}\hat{n}\cdot\mathbf{r}/r$.

The integrands of Eq. (3) have no singularities except the obvious one at $\tilde{r} = 0$, which will never occur in the far field. Therefore, it appears to be a simple matter to numerically integrate these well-behaved functions over the surface Σ. However, because the surface itself changes (sometimes rapidly) as a function of observer time, and because the surface area does not necessarily vary smoothly in the direction perpendicular to that of the motion (in this case, the radial direction), the integration requires careful consideration, particularly near critical points where $M_r = 1$ on leading and trailing edges of the surface. In the event of shock waves present on the blade surface, integration of the loading term would require the same consideration near points of $M_r = 1$ on the shock edge.

Several authors have pointed out the importance of the critical locations, but have been content to simply refine the integration grid in the vicinity of them. In fact, the area of the retarded planform changes so abruptly at points of sonic velocity in the observer direction that the planform must be considered discontinuous at that point. When the discontinuity of the planform is taken into account, the integral over it may be accurately and smoothly computed, and its numerical derivative easily follows. The physical reasoning for the discontinuous planform area is straightforward. At supersonic Mach number (relative to the observer), a single source in circular or helical motion produces signals at three distinct

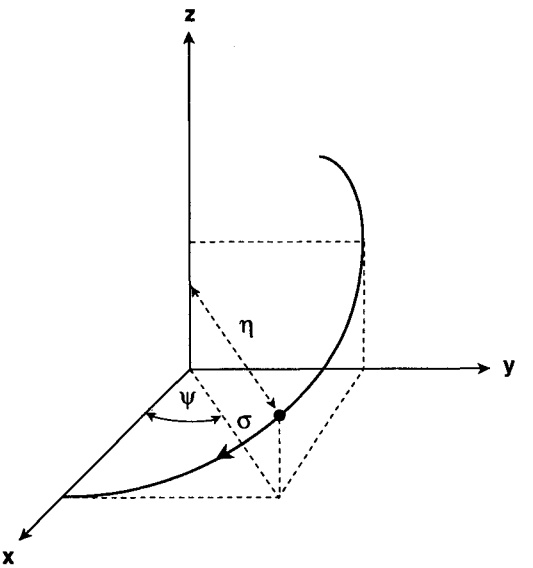

Fig. 3 Coordinate system for propeller in forward flight.

emission times which all reach the observer at the same observer time. The surface source acts as an assemblage of single sources, distributed between the leading and trailing edges of the surface. When the leading edge first becomes supersonic, the planform suddenly has increased area due to the fact that there are now three locations from which the sound is heard, rather than just one. Conversely, when an edge leaves the supersonic region, the number of locations of sound emission from that edge goes from three back to one. It can be imagined that whenever either edge passes through $M_r = 1$, the planform area at that point experiences a rapid change—in fact, a discontinuity.

The above can be shown more formally by considering an expression for the dimensionless area of the acoustic planform, which is simply

$$\tilde{A}(\tilde{t}) = \int\int d\Sigma \tag{4}$$

Introducing dimensionless coordinates η in the radial direction and σ in the helical direction (positive toward the trailing edge of the surface and negative in the direction of motion, as shown in Fig. 3), the equation becomes

$$\tilde{A}(\tilde{t}) = \int\int_{-\infty}^{\infty} [H(g - g_{le}) - H(g - g_{te})]\, d\sigma\, d\eta \tag{5}$$

where H represents the Heaviside step function and g is the retarding function equal to $\tilde{t} - \tilde{\tau} - \tilde{r}$. Integrating by parts

$$\tilde{A}(\tilde{t}) = -\int\int_{-\infty}^{\infty} \sigma[\delta(g - g_{le}) - \delta(g - g_{te})]\frac{dg}{d\sigma}\, d\sigma\, d\eta \tag{6}$$

In Eq. (6), δ represents the Dirac delta function. Completing the integration gives

$$\tilde{A}(\tilde{t}) = \int \left[\sum_n^{N_{te}} \sigma_n \frac{\dfrac{dg}{d\sigma}}{\left|\dfrac{dg}{d\sigma}\right|_n} - \sum_n^{N_{le}} \sigma_n \frac{\dfrac{dg}{d\sigma}}{\left|\dfrac{dg}{d\sigma}\right|_n}\right] d\eta \tag{7}$$

where the σ_n are the roots of $g(\sigma) = g_{le}$ or g_{te}. N_{le} and N_{te} refer to the total number of roots of g_{le} and g_{te}, respectively, More succinctly

$$\tilde{A}(\tilde{t}) = \int \left[\sum_n^{N_{te}} \sigma_n \operatorname{sgn}\left(\frac{dg}{d\sigma}\right)_n - \sum_n^{N_{le}} \sigma_n \operatorname{sgn}\left(\frac{dg}{d\sigma}\right)_n\right] d\eta \tag{8}$$

Thus, the area per unit radius (chord length) of the acoustic planform is simply a sum of the roots of the retarding function g. This is easily verified conceptually by realizing that g at a specified t and η, gives the locus of points from which the sound at that t originates. Therefore, if $g_{te} \leq g \leq g_{le}$, all points on the planform from which the sound originates at t will be included.

Figure 4 plots $g = g_{le}$ and $g = g_{te}$ for the SR3 propeller blade (as defined in Ref. 1) at a tip Mach number of 1.17 and a forward-to-tip speed ratio of 0.88. Note that the function is rearranged so that the plots show t vs $-\sigma$ for a given η (equal to the rotational Mach number at that radius). By plotting the function this way, the manner in which the planform area changes as a function of time is evident. In the figure, solid lines represent the trailing edge function and dashed lines the leading edge. The horizontal distance encompassed by the two lines is the chord length of the retarded surface at the specified η at the observer time of interest. The figure clearly shows the relationship between the chord and the roots of the retarding function, and the reason for including sgn(dg/dσ) in Eq. (8). With regard to the latter, in the case of one leading-edge root and three trailing-edge roots (case a in Fig. 4b), or, conversely, one trailing-edge root and three leading-edge roots (case b in Fig. 4b), the area between the two single-edge roots must also be considered. The middle root for a single edge will always have negative slope. Therefore, Eq. (8) will give the correct sign to that root. The zero-slope root for the special case when $\partial g/\partial\sigma = 0$ will also be assigned the correct value since such a location contributes no area to the planform.

To find the variation of the retarded area with respect to observer time, note that $\partial/\partial t = \partial/\partial g$. Taking this derivative of Eq. (8) gives

$$\frac{\partial}{\partial \tilde{t}}\tilde{A}(\tilde{t}) = \int \left[\sum_{n}^{N_{te}} \frac{1}{\left|\frac{dg}{d\sigma}\right|_n} + \sum_{n}^{N_{le}} \frac{1}{\left|\frac{dg}{d\sigma}\right|_n} \right] d\eta \qquad (9)$$

To recognize the significance of the above equation, consider the expression for M_r, the Mach number component in the direction of the observer

$$M_r = M_h \cdot \frac{\mathbf{r}}{|\mathbf{r}|} = -M_h\left(\hat{\sigma}\cdot\frac{\mathbf{r}}{|\mathbf{r}|}\right) \qquad (10)$$

M_h represents the total Mach number of the surface in the direction of motion (the helical direction). Now, recalling that $\tilde{r} = |\tilde{\mathbf{r}}| = |\tilde{x} - \tilde{y}|$, where $\tilde{x}$ is dimensionless observer location, $\tilde{y}$ is dimensionless source location, and $\partial\tilde{y}/\partial\tau = -M_h$, then

$$\frac{\partial \tilde{r}}{\partial \sigma} = \frac{1}{M_h}\frac{\partial r}{\partial \tau} = -\left(\hat{\sigma}\cdot\frac{\mathbf{r}}{|\mathbf{r}|}\right) \qquad (11)$$

Comparing Eq. (10) to Eq. (11), it can be seen that

$$M_h\left|\frac{dg}{d\sigma}\right| = |1 - M_r| \qquad (12)$$

which is a well-known result. Using Eq. (12) in Eq. (9), the time rate of change of the acoustic planform area becomes

$$\frac{\partial \tilde{A}}{\partial \tilde{t}} = M_h \int \left[\sum_{n}^{N_{te}} \frac{1}{|1 - M_r|_n} - \sum_{n}^{N_{le}} \frac{1}{|1 - M_r|_n} \right] d\eta \qquad (13)$$

As Eq. (13) indicates, the integrand of the area slope will have singularities whenever $M_r = 1$—the locations of the critical points. By considering the whole of Fig. 4, it can be seen that the singularity will occur at different times for adjacent radial positions, and that there will be at least one such critical location for any time that any part of the blade is

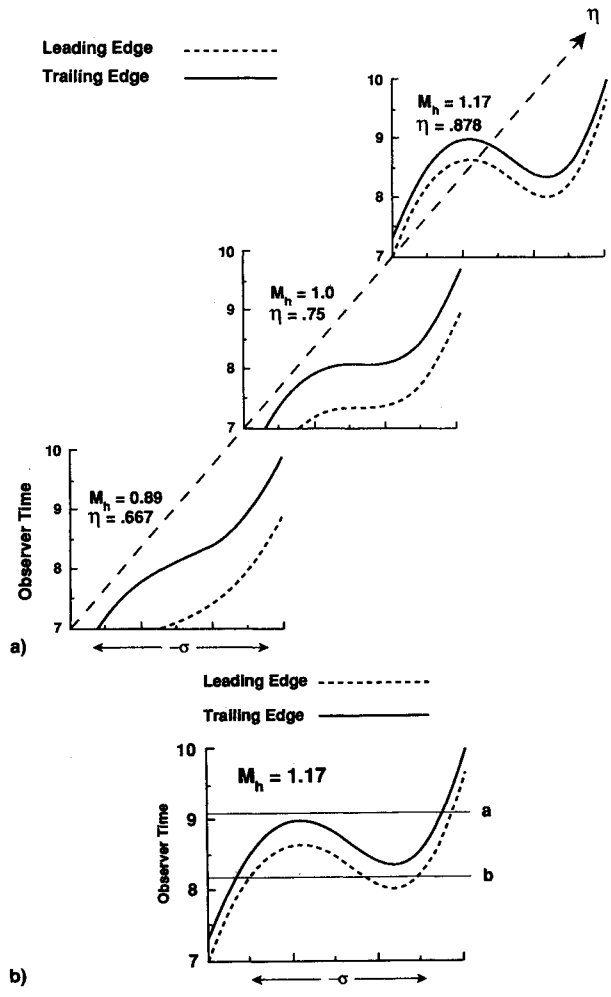

Fig. 4 Observer time vs chordwise position for various spanwise locations—solutions to $g = g_{le}$ and $g = g_{te}$.

traveling supersonically with respect to the observer. The $M_r = 1$ locations are shown to be points of true discontinuity in the retarded surface area, and it is crucial that they are treated as such in the integration. This requirement implies that, for each time at which the pressure is computed, the critical points must be determined. Therefore, a new integration grid must be specified for each observer time in the computation.

From Eq. (13), it appears that the acoustic planform area will exhibit a slope singularity at every time some edge travels at $M_r = 1$. However, keeping in mind that integrating tends to be a smoothing operation, it is found in practice that the integrated area over all spanwise stations has discontinuities only at times corresponding to points of true singularity when $M_r = 1$ and $M_N = 1$, as discussed above. The function $\tilde{A}(\tilde{t})$ will not exhibit singular behavior, but its derivative will have singularities at these times. Nonsingular discontinuities in the derivative do appear. These are discussed in Sec. III.

III. Discussion

The number and locations of the critical points at a given observer time depend heavily on the geometry of the rotating blade. As discussed previously, a straight blade will have one and only one critical point per edge per time. Swept blades, on the other hand, may have more than one critical point per edge, and the amount and type of sweep determine their number and location. It is easily seen that for a straight edge there can exist only one such point. Consider the in-plane case depicted in part a of Fig. 5. The blade edge lies along the line HA and the line of $M_r = 1$ locations lies along OA. If a pulse is produced by the edge at A, it will travel toward the observer at the speed of sound in the direction AO. The pulse will reach point B after a time given by the length AB

divided by the speed of sound. On the other hand, point C on the blade edge will reach point B after a time given by the length CB divided by the speed of sound. Since the length of CB is less than that of AB, a point on the blade edge along $M_r = 1$ will always be ahead of the sound it produced at an earlier time. There will, therefore, never be more than one emission at $M_r = 1$ at a given observer time.

Part b of Fig. 5 illustrates a possible scenario for a curved blade edge. Again the blade edge HA emits a signal at point A, which travels toward the observer at the speed of sound along AO. The sound reaches point B after a time $|AB|/\alpha_0$, whereas the blade reaches location B after a time $|A'B'|/\alpha_0$. It can be seen that $|A'B'|$ is less than $|AB|$ so that, as in the case of the straight blade, the blade out-distances its sound and only one critical point occurs per observer time. However, during the second half of the supersonic sweep (i.e., most of the second quadrant), the opposite conditions occur. If the blade edge emits a signal at point B, the pulse travels toward the observer and reaches point C after time, $|BC|/\alpha_0$. The blade reaches point C after time $|B'C'|/\alpha_0$ which, as drawn, is greater than the pulse time. Therefore, there is some time when the pulse time and the blade time are exactly the same,

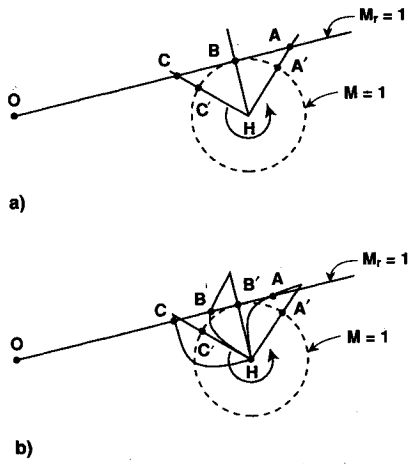

Fig. 5 Location of critical points by emission at $M_r = 1$: a) straight-blade edge, and b) swept-blade edge.

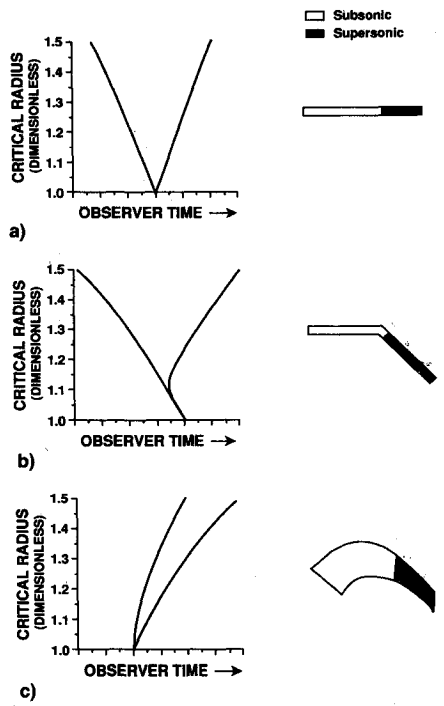

Fig. 6 Spanwise critical point locations for a single edge: a) straight blade, b) straight blade with straight sweep on outer 33%, and c) propfan-type blade.

which leads to two critical points on the edge for that observer time. It is possible to have more than two critical points, the exact number depends on the edge sweep and the tip Mach number. Figure 6 shows the positions of the critical points vs observer time for three blade shapes. Though the above discussion is given for a rotor with no axial velocity and with in-plane observer, the results for a blade in helical motion with observer out of plane are similar.

It is interesting to examine the actual retarded shapes (acoustic planforms) over which the integration is performed. Figure 7 shows a sequence of planforms for a straight blade in hover with a tip Mach number of 1.2. A significant feature as the series develops is that the planform becomes disconnected; this begins to occur at the time when the blade first becomes supersonic with respect to the observer. Note that the total area of the planform experiences a rapid rise at such a time. This leads to a discontinuity in the computed acoustic waveform—a condition which Amiet termed a "near-singularity." Near-singularities, or discontinuities, occur whenever the blade tip moves on or off the $M_r = 1$ line, since these times correspond to an instantaneous change in the growth rate of the planform area. The discussion in Sec. II refers briefly to these near-singularities in the context of the time derivative of the acoustic planform area.

Figure 8 shows a progression of acoustic planforms projected onto the plane of rotation for a propfan-type blade. The blade is in forward flight with advance ratio $V_f/\Omega R$ equal

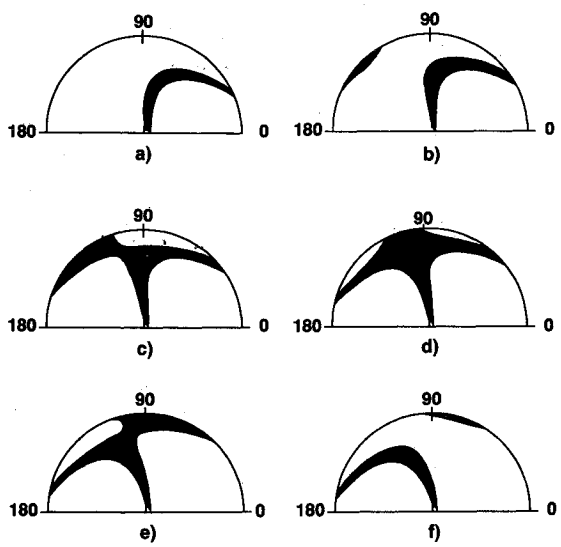

Fig. 7 Acoustic planforms for straight blade in hover, $M_{tip} = 1.2$: a–f) increasing observer time.

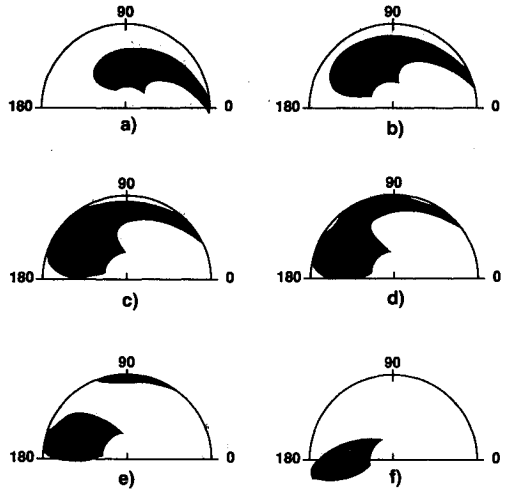

Fig. 8 Acoustic planforms for propfan-type blade, helical tip Mach number = 1.17, $V_f/\Omega R = 0.88$: a–f) increasing observer time.

to 0.88, and with helical tip Mach number equal to 1.17. The figure clearly illustrates the effect of sweep on the retarded shape. One important difference from the straight blade is that there is no near-singularity produced at the beginning of the supersonic portion of the cycle. For highly swept blades, the radial location near $M_h = 1$ (with M_h equal to the helical Mach number) produces the sonic signal first heard by the observer. This is shown in Fig. 6c for this type of blade. When this initial supersonic signal is produced inboard, the planform grows smoothly, as illustrated in Fig. 8, and no discontinuity in the growth rate of the planform area occurs. The final sonic signal heard by the observer is produced by the trailing edge tip (again, see Fig. 6), and at this time a discontinuity will be produced. Notice, also, that the planform becomes disconnected near the end of the supersonic part of the cycle—this is one of the phenomena which has been shown to cause the abrupt change in planform area.

Figure 9 gives some three-dimensional views of a propfan rotor blade acoustic planform. Note that all views in this figure represent the same planform (at the same observer time). Views (a–f) show rotations about a horizontal axis through a total of almost 180 degrees. The planform corresponds to that shown in Fig. 8a—there is one leading-edge critical point. The helices traced by the blade root and tip are also illustrated.

Figure 10 shows a thickness noise waveform for the propfan blade with a parabolic arc airfoil whose thickness varies linearly along the span, tapering to 2% thick at the tip. The leading edge of the blade has a greater amount of sweep than the trailing edge, so that the trailing edge produces a singularity in the waveform and the leading edge does not. Another characteristic of note is that there is no near-singularity at the beginning of the pressure pulse, an expected result in light of the interpretation of Figs. 6 and 8. The waveform is perfectly smooth except at the singularity and at the near singularity at the end of the pulse.

To compute the loading noise, the Δp on the blade is required. This data is not readily available, but some general conclusions regarding the expected loading noise waveform can be drawn based on the previous discussion. If the pressure loading ($\Delta p = p_{\text{lower}} - p_{\text{upper}}$) is smooth and equal to zero at the leading and trailing edges, the source integrand will have no discontinuities and no singularities are expected in the far field. Additionally, no near-singularities are expected since their existence depends on the value of the source being nonzero at the edges. If, on the other hand, a Δp such as that calculated from linearized supersonic airfoil theory is used, the pressure loading will have discontinuities similar to those found in the thickness integrand. Therefore, singularities of the same type exhibited by the thickness noise waveform should

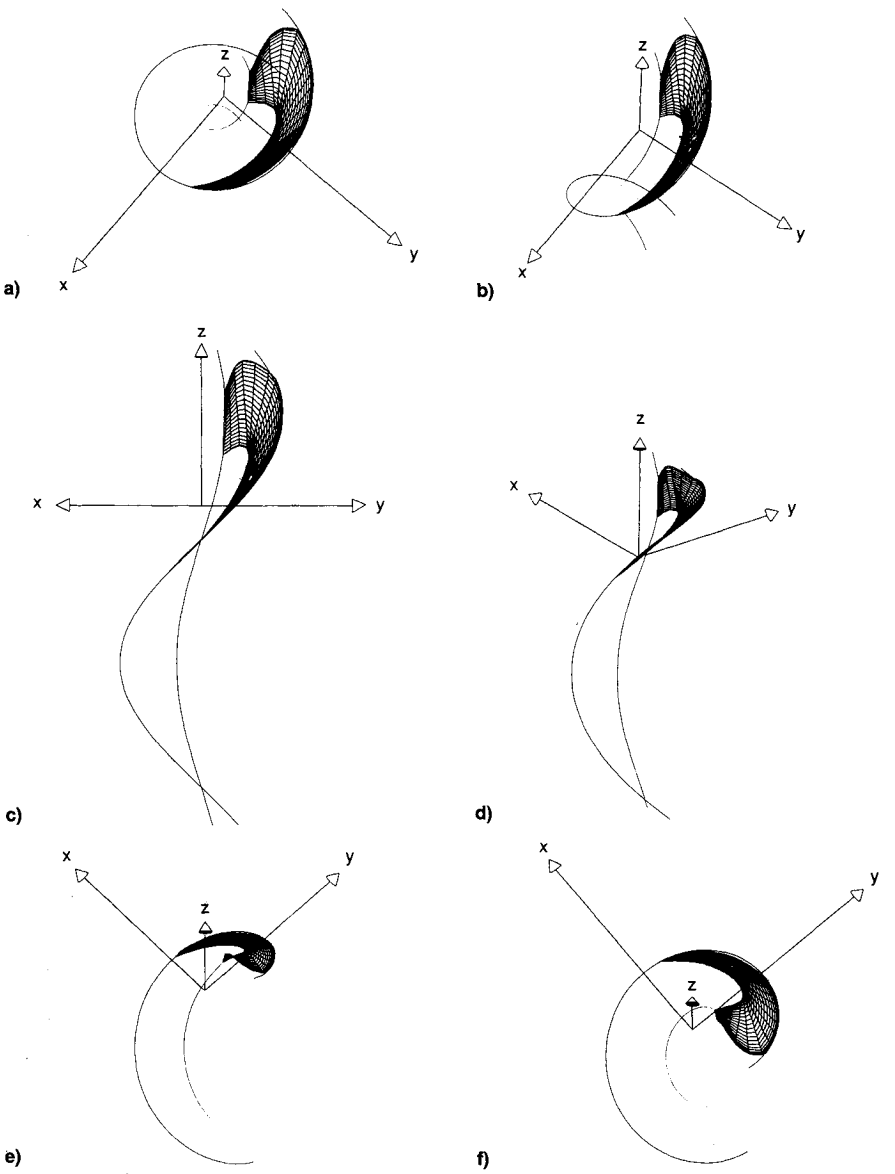

Fig. 9 Acoustic planforms, propfan-type blade, one leading-edge critical point: a–f) change of viewpoint.

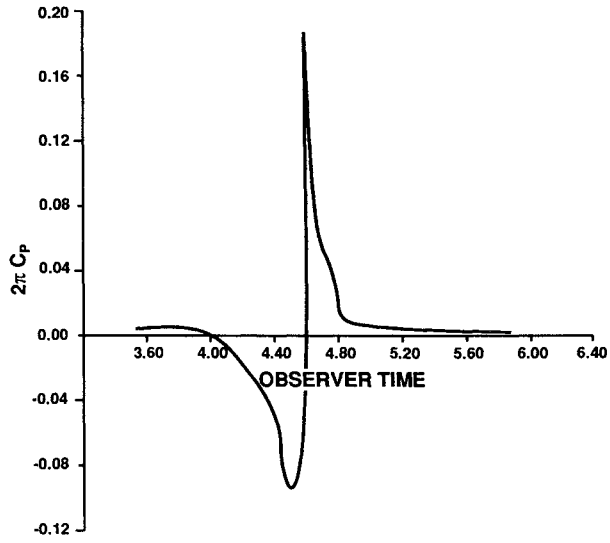

Fig. 10 Thickness noise (dimensionless) vs observer time (dimensionless)—propfan-type blade.

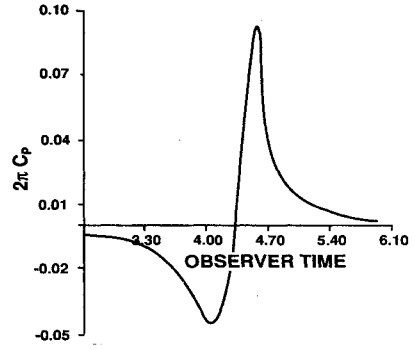

Fig. 11 Loading noise (dimensionless) vs observer time (dimensionless)—propfan-type blade, $\Delta p = 0$ at edges.

appear. This predicted behavior is, in fact, borne out by the computations. Figure 11 shows the loading noise predicted using a parabolic pressure loading on the blade. In this case, $\Delta p = 0$ at the leading and trailing edges, and as expected, no sigularities appear in the computed waveform.

IV. Conclusions

The developed methodology for computing acoustic pressure for rotating blades with supersonic tips produces smooth waveforms for all blade geometries tested. In particular, the waveforms computed for the complex geometry of the propfan-type blades are completely smooth except at points of singularity or discontinuity, where smoothness is not expected. The method appears to be quite efficient relative to other formulations, though no exact comparisons have been carried out. A high efficiency is expected since the current method does not require numerical integration of singular (but integrable) integrands, and can therefore make do with fewer integration points. The accuracy of the integrations is ensured by recognizing the area-per-unit-span discontinuity of the retarded planform at the critical points of $M_r = 1$. Treating the integrals in this way produces a smooth curve which is readily numerically differentiated. Because of the numerical differentiation, the described method will likely require more time steps than the methods which take the derivative inside the integral sign.

The advanced geometry of the propfan introduces some interesting complexities to the calculation. Whereas straight blades, such as those of helicopters, will have only one critical point per edge per observer time, blades with swept edges will often have two such points, and can have as many as four critical points per edge per observer time. The number of points depends on the amount and type of sweep—highly swept edges will tend to have two critical points per edge at a given time, while edges with less or variable sweep will usually have more. The critical locations—where $M_r = 1$—are important since they represent the points of discontinuity in the spanwise integration over the acoustic planform. Related to the change in number and location of critical points is a change in number and location of near-singularities or discontinuities in the computed waveforms. These occur when the tip edges enter or leave the supersonic region (with respect to the observer). At these times, the growth rate of the acoustic planform area changes abruptly which leads to the instantaneous change in slope of the waveform.

Singularities in the propagating wave are produced by the rotating blade if a point on the blade edge is simultaneously moving toward the observer at $M_r = 1$ and the Mach number normal to its edge is 1. The singularity will only occur if there is a discontinuity in the source integrand at the edge. Thus, thickness sources, which will always have discontinuities at leading and trailing edges for normal airfoil shapes, will always produce singularities if the above conditions hold. The singularity is logarithmic. The loading noise waveform may have singularities if the Δp distribution along the airfoil is discontinuous at the edges, as in the distribution predicted by supersonic thin airfoil theory. The singularities (and near singularities) should occur at the same observer time as those in the thickness waveform. On the other hand, if the Δp distribution over the airfoil is smooth and equal to zero at the leading and trailing edges, no singularities are expected. In both thickness and loading cases, sweep delays the appearance of the singularity since it reduces the magnitude of the Mach number normal to the blade edge. The current computations bear out all of the above expectations.

References

[1]Farassat, F., Dunn, M. H., and Padula, S. L., "Advanced Turboprop Noise Prediction Based on Recent Theoretical Results," *Journal of Sound and Vibration*, Vol. 119, Nov. 1987, pp. 53–79.

[2]Hanson, D. B., "Near-Field Frequency-Domain Theory for Propeller Noise," AIAA Paper 83-0688, April 1983.

[3]Amiet, R. K., "Thickness Noise of a Propeller and Its Relation to Blade Sweep," *Journal of Fluid Mechanics*, Vol. 192, July 1988, pp. 535–560.

[4]Chapman, C. J., "Shocks and Singularities in the Pressure Field of a Supersonically Rotating Propeller," *Journal of Fluid Mechanics*, Vol. 192, July 1988, pp. 1–16.

[5]Wells, V. L., "Integrating the Acoustic Analogy for Supersonic Rotating Surfaces," AIAA Paper 89-1133, April 1989.

[6]Farassat, F., "Theoretical Analysis of Linearized Acoustics and Aerodynamics of Advanced Supersonic Propellers," AGARD-CP-366, Nevilly SurSeine, France, 1985, pp. 10-1–10-15.

[7]Farassat, F., "Prediction of Advanced Propeller Noise in the Time Domain," *AIAA Journal*, Vol. 24, April 1986, pp. 578–584.

[8]Farassat, F., and Brentner, K. S., "The Uses and Abuses of the Acoustic Analogy in Rotor Noise Prediction," *Journal of the American Helicopter Society*, Vol. 33, Jan. 1988, pp. 29–36.

[9]Farassat, F., "Quadrupole Source in Prediction of the Noise of Rotating Blades—A New Source Description," AIAA Paper 87-5225, Oct. 1987.

[10]Wells, V. L., "Acoustic Waveform Singularities from Supersonic Rotating Surface Sources," *AIAA Journal*, Vol. 29, March 1991, pp. 387–394.

[11]Chapman, C. J., "Whitham's F-Function in Supersonic Propeller Acoustics," AIAA Paper 89-1107, April 1989.

[12]Lighthill, M. J., "On Sound Generated Aerodynamically. I. General Theory," *Proceedings of the Royal Society, Series A*, Vol. 221, 1952, pp. 564–587.

[13]Tam, C. K. W., "On Linear Acoustic Solutions of High Speed Helicopter Noise Problems," *Journal of Sound and Vibration*, Vol. 89, July 1983, pp. 119–134.

[14]Farassat, F., "Theory of Noise Generation from Moving Bodies with an Application to Helicopter Rotors," NASA TR R-451, Dec. 1975.

[15]Ffowcs Williams, J. E., and Hawkings, D. L., "Sound Generation by Turbulence and Surfaces in Arbitrary Motion," *Philosophical Transactions of the Royal Society of London, Series A*, Vol. 264, May 1969, pp. 321–342.